

STUDY OF TROPOSPHERIC AEROSOL PROPERTIES OVER CHIBA, JAPAN USING MULTI-WAVELENGTH LIDAR, SUN PHOTOMETER, AND METEOROLOGICAL DATA

○Taisuke Oshima¹, Shunsuke Fukagawa¹, Nobuo Takeuchi¹, Hiroaki Kuze¹, Gerry Bagtasa¹,
Suekazu Naito², Masanori Yabuki³

¹*Center for Environmental Remote Sensing, Chiba University,*

²*Chiba Prefectural Environmental Research Center,* ³*National Institute of Polar Research*

Abstract:

Tropospheric aerosol properties are studied in Chiba, Japan, by means of ground-based sun-photometer and multi-wavelength lidar observations. Vertical profiles of aerosol extinction coefficient are derived from the continuous measurement using a multi-wavelength (355, 532, 756, 1064 nm) lidar system. It is found that the temporal variation of the aerosol extinction near the ground layer often exhibits some correlation with that of relative humidity, wind speed, and wind direction measured at the ground level. Also, information on the aerosol size distribution can be retrieved from the Angstrom exponent calculated from the lidar data and sun-photometer data.

1. Introduction

Combinatory measurements with a lidar and conventional instruments provide detailed information on aerosol properties from the ground level to the upper atmosphere. Over the Kanto plain area (large Tokyo metropolitan area), for example, an inter-comparison experiment was conducted during the ACE-Asia intensive observation period,¹⁾ investigating the occurrence of a large-scale yellow sand event by comprehensive measurements with lidars, sun photometers, as well as with concurrent aircraft measurements.

At the Center for Environmental Remote Sensing

(CEReS), Chiba University, aerosol studies based on ground sampling and optical monitoring have been undertaken.²⁻⁵⁾ Ground instruments including an integrated nephelometer, an optical particle counter, and a scatterometer based on an integrating sphere⁴⁾ have provided aerosol data at the ground level, in conjunction with the monthly data from the chemical sampling and the daytime data with a sun photometer.⁵⁾ Although these methods give information of aerosols at the ground level and through the entire atmosphere (in the form of the optical thickness), the vertical variation, or the profile, of aerosol particles that is obtained from lidar measurements is indispensable for the proper understanding of regional aerosols.

As shown in Fig. 1, the campus of Chiba University is located on the east side of the Tokyo Bay, surrounded by urban (dark gray) and agricultural/forest (grey) regions. This location provides us with the possibility of observing various aerosols in accordance with the regional wind conditions. In the present paper,

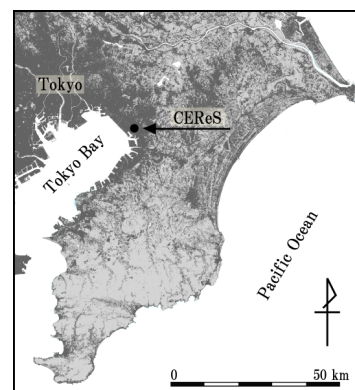


Fig.1 Location of CEReS, Chiba University

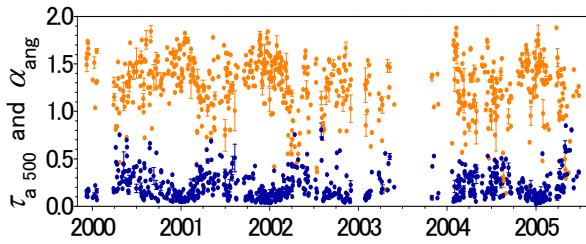


Fig.2 Long-term Variation of AOT and α_{ang}

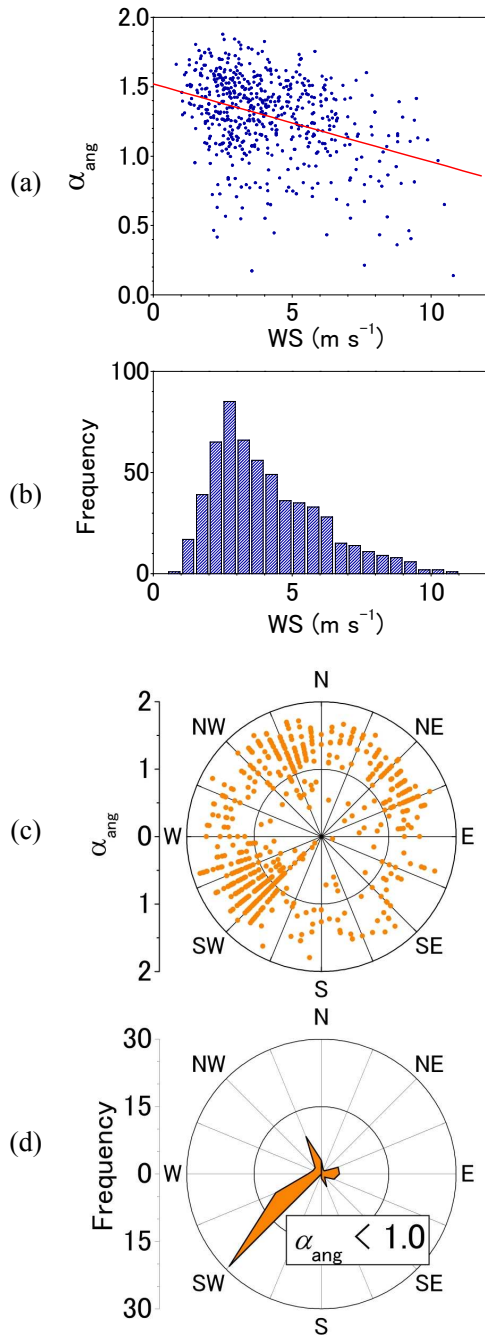


Fig.3 Relationship between α_{ang} and wind.

we describe aerosol properties of the Chiba area derived mainly from the long-term sun-photometer data and recent observations using a multi-wavelength lidar system.

2. Sun-photometer observation

Aerosol optical thickness (AOT) over the Chiba area has been measured between 1999 and 2005, with 4 wavelength bands centered at 368, 500, 675, and 778 nm. After the correction of Rayleigh, ozone, and air-mass effects, the vertical (column) value of AOT at a wavelength $\lambda_0=500$ nm is calculated using the following equation:

$$\tau(\lambda) = B (\lambda_0 / \lambda)^{\alpha_{ang}} \quad (1)$$

The resulting long-term variations of the AOT (500 nm) and the Angstrom exponent α_{ang} are plotted in Fig. 2. From the location of the CERES site, it is interesting to examine the influence of the wind system on the aerosol properties. The relation between the wind speed/direction and the Angstrom exponent is shown in Fig. 3. Figure 3(a) indicates a negative correlation between the wind speed and α_{ang} , suggesting the dominance of coarse particles (with diameter $d > 2 \mu\text{m}$) under strong winds. From Fig. 3(c) and (d), it is seen that the southwest wind direction gives rise to $\alpha_{ang} < 1$: hence, such coarse particles are ascribable to sea-salt particles from the sea region.

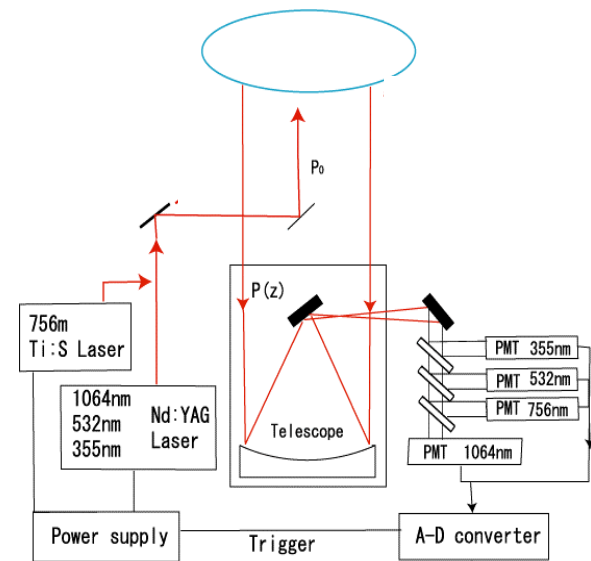


Fig.4 Schematic diagram of multi-wavelength lidar.

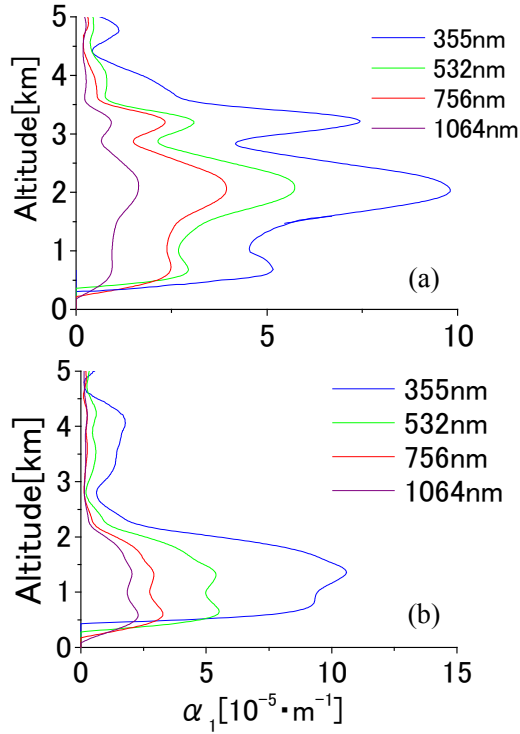


Fig.5 Extinction profiles observed in (a) summer (18:09:21 JST on 19 August 2005) and (b) winter (20:38:15 JST on 17 November 2005). (Show time stamps of observations here)

3. Observations with a multi-wavelength lidar

A schematic drawing of the multi-wavelength, Mie-scattering lidar system is shown in Fig. 4. Two Nd:YAG lasers and a Ti:Sapphire laser are employed to produce the 4 wavelength with 10 Hz pulse repetition rate. The diameter of the main mirror of the Newtonian telescope is 80 cm, and 4 photo-multipliers are used to detect the lidar signals.

Under the assumption of the single scattering, the signal received by a Mie-scattering lidar can be given as:

$$P(z) = C \frac{G(z)}{z^2} [\beta_a(z) + \beta_m(z)] \times \exp \left[-2 \int_{z_0}^z \alpha_a(z') dz' - 2 \int_{z_0}^z \alpha_m(z') dz' \right] \quad (2)$$

where z is the altitude, $\alpha(z)$ is the extinction coefficient, $\beta(z)$ is the backscattering coefficient, C is the system constant, and $G(z)$ is the overlapping function. Suffices “a” and “m” refer to aerosols and air molecules,

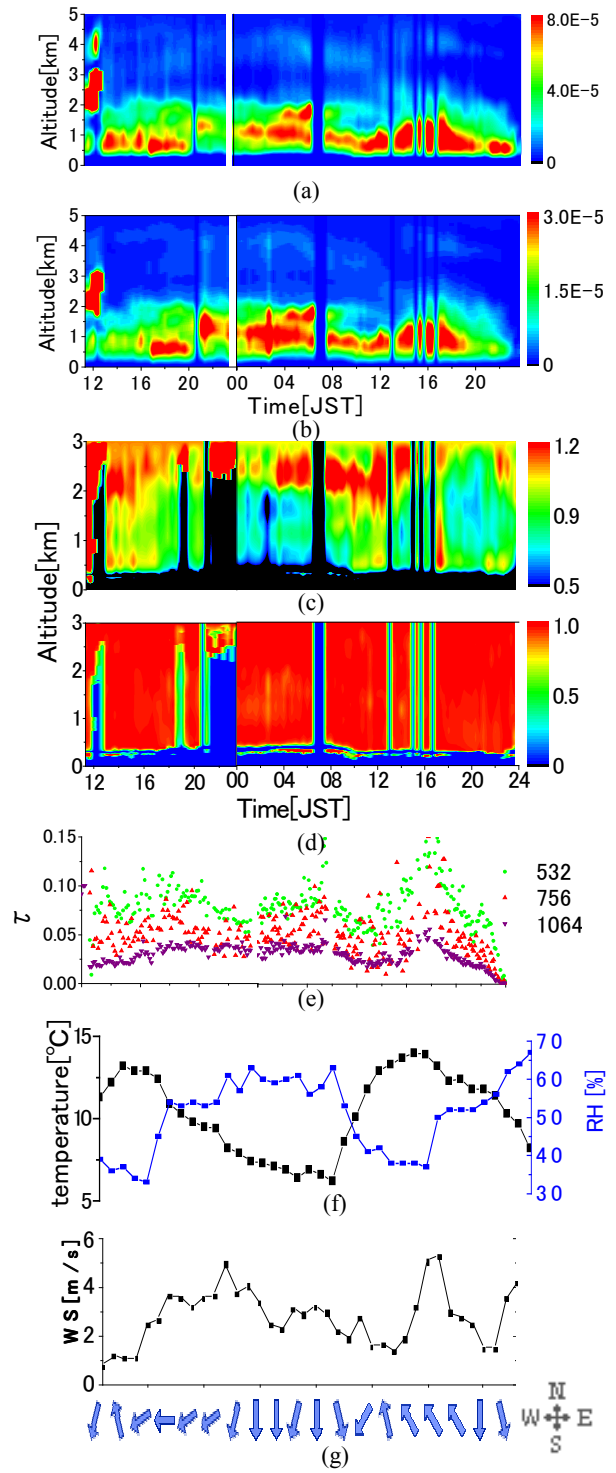


Fig.6 Lidar and meteorological data observed on 17-18 November 2005: (a) aerosol extinction profile for 532 nm, (b) the same for 1064 nm, (c) Angstrom exponent (AE), (d) correlation for determination of AE, (e) lidar-derived AOT for 532, 756 and 1064 nm (f) air temperature and RH, and (g) wind field.

respectively. The aerosol extinction profile, $\alpha_a(z)$, is derived by solving Eq.(2) using the Fernald's method⁶⁾ with $S_1 = 54.7, 53.0, 46.0$ and 43.2 sr for each lidar wavelength (355, 532, 756, and 1064 nm, respectively) as predicted from the Chiba winter model.⁷⁾ In solving Eq. (2), the boundary value for 532 nm at a reference altitude of 5.5 km is obtained from the aerosol profile model in Chiba that has been derived from the portable, automated lidar (PAL) data.⁸⁾

Typical aerosol profiles obtained in summer and winter are shown in Fig. 5(a) and (b), respectively. In the summer case, aerosol layers are seen centered around 2 km above ground level (AGL). In the winter case, on the other hand, the layer is more compact and its height is centered around 1.5 km AGL.

Figure 6 shows an example of time-height indications of extinction profiles for two wavelengths (532 and 1064 nm) and the profile of the Angstrom exponent (determined from all the 4 wavelengths), together with the temporal changes of temperature, relative humidity (RH), wind speed, and wind velocity observed on 17-18 November 2005. From this figure, it is seen that the aerosol extinction coefficient profiles up to several km AGL, and in particular, that in the altitude range of 1-2 km, are correlated with the changes in RH and wind speed.

From the lidar-derived profile of the Angstrom exponent (Fig. 6(c)), it is seen that relatively large aerosols with α_{ang} below 1 are dominant in the altitude range up to 1.5 km, whereas an aerosol layer with slightly smaller particles (with α_{ang} around 1.2) appears around the altitude of 2.5 km. Details about the relationship between the lidar profile and the ground-measured data will be discussed in the presentation.

As compared with the ACE-Asia experiment¹⁾ mentioned above, the present study has dealt with more regional and detailed properties of urban aerosols that are undisturbed with outside sources (such as the yellow sand). This type of aerosol study in conjunction

with the regional climate conditions gives us the basis for atmospheric correction study of satellite remote sensing data and for regional study of the radiation budget in the atmospheric environment.

References

1. T. Murayama et al., An intercomparison of lidar-derived aerosol optical properties with airborne measurements near Tokyo during ACE-Asia, *J. Geophys. Res.*, 108(D23), 8651, doi:10.1029/2002JD003259 (2003).
2. M. Yabuki, H. Kuze, H. Kinjo, N. Takeuchi, Determination of vertical distributions of aerosol optical parameters by use of multi-wavelength lidar data, *Jpn. J. Appl. Phys.*, 42(1) 686-694 (2003).
3. N. Lagrosas, H. Kuze, N. Takeuchi, S. Fukagawa, G. Bagtasa, Y. Yoshii, S. Naito, M. Yabuki, Correlation study between suspended particulate matter and PAL, *Aerosol Science* 36, 439-454 (2005).
4. S. Fukagawa, H. Kuze, N. Lagrosas, N. Takeuchi, High-efficiency aerosol scatterometer that uses an integrating sphere for the calibration of multiwavelength lidar data, *Appl. Opt.*, 44, 3520-3526 (2005).
5. S. Fukagawa, H. Kuze, G. Bagtasa, S. Naito, M. Yabuki, T. Takamura, N. Takeuchi, Characterization of seasonal and long-term variation of tropospheric aerosols in Chiba, Japan, *Atmospheric Environment*, in press (available online) (2006).
6. F.G.Fernald, Analysis of atmospheric lidar observations: some comments *Appl. Opt.* Vol.23, No.5, pp. 652-653, (1984)..
7. M. Yabuki, Study on algorithms for deriving optical parameters of tropospheric aerosol (in Japanese), Ph.D. thesis, Chiba University (2003).
8. S. Fukagawa, Long-term measurement of atmospheric aerosol properties and improvement in its accuracy, (in Japanese), Ph.D. thesis, Chiba University (2006).